https://doi.org/10.15407/ujpe67.9.631

M.G. SRINIVAS,[1,2] H.C. MANJUNATHA,[3] K.N. SRIDHAR,[1] A.C. RAJ,[2]
P.S. DAMODARA GUPTA [3]

[1] Department of Physics, Government First Grade College
(Mulbagal-563131 Karnataka, India)
[2] Department of Physics, St. Joseph's college (autonomous),
Affiliated to Bharathidasan University
(Tiruchirappalli-620002, Tamilnadu, India)
[3] Department of Physics, Government College for Women
(Kolar-563101 Karnataka, India; e-mail: manjunathhc@rediffmail.com)

A SYSTEMATIC STUDY OF PROTON DECAY IN SUPERHEAVY ELEMENTS

We have studied the proton decay in almost all superheavy nuclei with atomic number $Z = 104$–126. We have calculated the energy released during the proton decay (Q_P), penetration factor (P), normalization factor (F), and the proton decay half-lives. The latter are also longer than that of other decay modes such as the alpha decay and spontaneous fission. The competition of the proton decay with different decay modes reveals that the proton decay is not the dominant decay mode in the superheavy nuclei region. This means that superheavy nuclei are stable against the proton decay.

Keywords: radioactivity, superheavy nuclei, proton decay.

1. Introduction

The phenomenon of the proton emission from nuclear ground states limits the possibilities of the creation of more exotic proton-rich nuclei that are usually produced by fusion-evaporation nuclear reactions. In the energy domain of radioactivity, a proton can be considered as a point charge having the highest probability of being present in the parent nucleus. Goncallves *et al.* [1] studied the two-proton radioactivity of nuclei of the mass number $A < 70$ using the effective liquid drop model. Delion *et al.* [2] reviewed the theories of proton emission to analyze the properties of nuclear matter. Maglione *et al.* [3] analyzed the proton emission from the some deformed nuclei. Delsanto *et al.* [4] investigated the β-delayed proton emission of ^{69}Kr and ^{68}Se and extracted their proton separation energies, half-lives and excitation energies. Alavi *et al.* [5] calculated the proton radioactivity half-lives of 45 proton emitters by the WKB method and observed a decrease in the values of calculated half-lives using the orientation angle-dependent formalism. Raciti *et al.* [6] measured the emission of two protons from the decay of ^{18}Ne excited states. Baye *et al.* [7] studied that a proton is emitted during β decay of one neutron halo nuclei. Feix *et al.* [8] computed the decay widths of proton emission for $Z = 51$ to 71 nuclei using the droplet model potentials and spectroscopic data from the shell model considerations. Anguiano *et al.* [9] investigated the photo-emission of two protons from ^{12}C, ^{16}O, and ^{40}Ca nuclei for the study of short-range correlations. Coniglione *et al.* [10] explored high-energy proton emission in heavy ion reactions close to the Fermi energy by investigating the production mechanism of energetic protons in an experiment performed with a MEDEA detector.

Giusti *et al.* [11] developed the theoretical framework of the emission of two protons in electron-induced reactions. Ludewigt *et al.* [12] studied the proton emission in alpha-induced reactions at 43 MeV per nucleon. Guzman *et al.* [13] analyzed the proton emission from proton-rich nuclei and calculated the half-lives using the effective liquid drop model. Delion *et al.* [14] also studied the proton emission. Dong *et al.* [15] theoretically calculated the half-lives of proton emitters using a generalized liquid drop model (GLDM) and the WKB approximation. Enrico Maglione *et al.* [16] studied the proton emission from ^{125}Pm and discussed the behavior of half-lives as a function of the deformation, spin of the decaying state, and energy of the emitted protons. Arumugam *et al.* [17] investigated the proton emission, gamma deformation, and the spin of the isomeric state of ^{141}Ho and revealed that the proton emission measurements could be a precise tool to probe triaxial deformations and other structural properties of exotic nuclei beyond the proton drip-line. Duarte *et al.* [18] studied the half-lives for the proton emission, alpha decay, cluster radioactivity, and cold fission processes theoretically. Ferreira *et al.* [19] also studied the proton radioactivity from spherical nuclei theoretically using a relativistic density functional derived from the meson exchange and point coupling The literature surveys testify that there is a lack of studies of the proton emission from superheavy nuclei. Superheavy nuclei are unstable and decay through various decay modes. In the present work, we will consider the proton emission from superheavy nuclei.

2. Theoretical Framework

The half-live for the proton emission is calculated using the equation

$$T_{1/2} = \frac{h\ln(2)}{2\pi\Gamma}, \tag{1}$$

where Γ is the decay width and is calculated using the relation

$$\Gamma = \frac{S\bar{F}h^2\bar{P}}{16\pi^2 m}. \tag{2}$$

Here, S, F, and P are spectroscopic, normalization, and penetration factors, respectively, $\bar{F}$ is the average normalization factor

$$\bar{F} = \frac{2}{\pi}\int\limits_0^{\pi/2} F(\theta)d\theta, \tag{3}$$

where $F(\theta)$ is the angle-dependent normalization factor

$$\bar{P} = \int\limits_0^{\pi/2} P(\theta)\sin\theta d\theta. \tag{4}$$

Here, $P(\theta)$ is the angle-dependent penetration factor. In the present work, the semiclassical WKB method is used to calculate the angle-dependent penetration factor, $P(\theta)$, and the angle-dependent normalization factor, $F(\theta)$ [20]:

$$F(\theta) = \frac{1}{\frac{1}{2}\int_{r_1(\theta)}^{r_2(\theta)}\frac{1}{k(r,\theta)}\,dr}, \tag{5}$$

$$P(\theta) = \exp\left[-2\int\limits_{r_2(\theta)}^{r_3(\theta)} k(r,\theta)\,dr\right]. \tag{6}$$

In the above relations, $r_1(\theta)$, $r_2(\theta)$, and $r_3(\theta)$ are the classical turning points at each angle which are defined as the roots of $Q - V(r,\theta) = 0$ and $r_1(\theta) < < r_2(\theta) < r_3(\theta)$. Here, $k(r,\theta)$ is calculated using the relation

$$k(r,\theta) = \sqrt{\frac{8\pi^2 m}{h^2}[Q - V(r,\theta)]}, \tag{7}$$

where Q is the energy released during the proton emission, and V is the total potential which is taken as the sum of the nuclear, spin-orbit, Coulomb, and centrifugal terms

$$V = V_N + V_{\text{spin-orbit}} + V_{\text{coul}} + V_L \tag{8}$$

Nuclear potential V_N is calculated using the equation

$$V_N = -V_R f(r,R,a)$$

with

$$V_R = -\left[47 - 0.46\frac{Z}{A^{1/3}} + 38\frac{(A-2Z)}{A}\right]\ \text{MeV}, \tag{9}$$

where $f(r,R,a) = \frac{1}{1+e^{(r-R)/a}}$ with $R = 1.17A^{1/3}$ Coulomb term is considered as

$$V_C = \begin{cases} \left(\frac{Ze^2}{8\pi\epsilon_0 R_c}\right)\left(3 - \frac{r^2}{R_C^2}\right) & r \le R_c, \\ \frac{Ze^2}{4\pi\epsilon_0 r} & r > R_c, \end{cases} \tag{10}$$

Table 1. **List of studied superheavy nuclei for proton decay**

Z	Mass number of Studied isotopes	Mass number of isotopes for which Q_P is $+V_e$
104	240–339	240
105	241–339	241–251
106	244–339	240–243
107	247–339	247–257
108	250–339	250–253
109	253–339	253–263
110	256–339	256–261
111	259–339	259–267
112	262–339	262–265
113	266–339	266–276
114	269–339	269–271
115	272–339	272–280, 291
116	275–339	275–279
117	278–339	278–287, 291
118	281–339	281–285
119	284–339	284–296
120	287–339	287–292
121	290–339	290–303
122	294–339	294–299
123	297–339	297–309
124	300–339	300,301
125	303–339	303–315
126	306–339	308–329

where $R_C = 1.21(A_d)^{1/3}$ in the present work is taken as

$$V_{\text{spin}-\text{orbit}} = V_{\text{SO}}(\boldsymbol{\sigma}\,\mathbf{L})\lambda_\pi^2 \frac{1}{r}\frac{d}{dr} f(r, R_{\text{SO}}, a_{\text{SO}}). \qquad (11)$$

Here, $R_{\text{SO}} = 1.01A^{1/3}$, $a_{\text{SO}} = 0.75$, (all of the lengths are in fermi), $V_{\text{SO}} = 6.2$ MeV, $m = A/A+1$, $\lambda_\pi^2 \approx \approx 2.0$ fm^2, and σ is the three-dimensional Pauli matrix

$$\boldsymbol{\sigma}\,\mathbf{L} = \begin{cases} L \quad \text{for} \quad j = L + \dfrac{1}{2}, \\ -(L+1) \quad \text{for} \quad j = L - \dfrac{1}{2} > 0. \end{cases} \qquad (12)$$

The centrifugal term is taken as

$$V_L = L(L+1)\frac{h^2}{8\pi^2 \mu r^2}, \qquad (13)$$

where

$$\mu = \frac{A}{A+1}.$$

3. Results and Discussion

The energy released during the proton decay (Q) is calculated using the difference of mass excess values available in the literature. We have used experimental mass excess values [21]. For those nuclei, where experimental mass excess was unavailable, we have used recent theoretical values [22, 23]. The list of studied superheavy nuclei with the proton decay is given in the Table 1. In this table, we have highlighted the nuclei for which the proton decay is possible. The energy released during the proton decay (Q_P), penetration factor (P), normalization factor (F), and logarithmic half-lives for the proton decay of superheavy nuclei are also given in Table 2.

To study the competition between different decay modes, we have also calculated the alpha decay half-lives and spontaneous fission half-lives. Alpha decay half-lives are evaluated using the semiempirical relations given by Royer [24], UNIV [25], NRDX [26], and Denisov [27]. Spontaneous fission half-lives are evaluated using semiempirical formula given by Xu *et al.* [28]. Figure 1 shows the competition between dif-

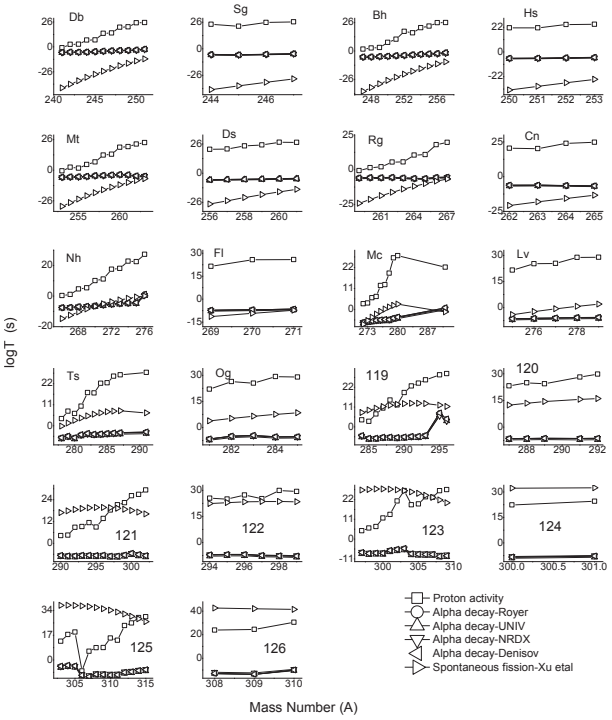

Fig. 1. Competition between different decay modes such as proton decay, spontaneous fission, and alpha decay for superheavy elements

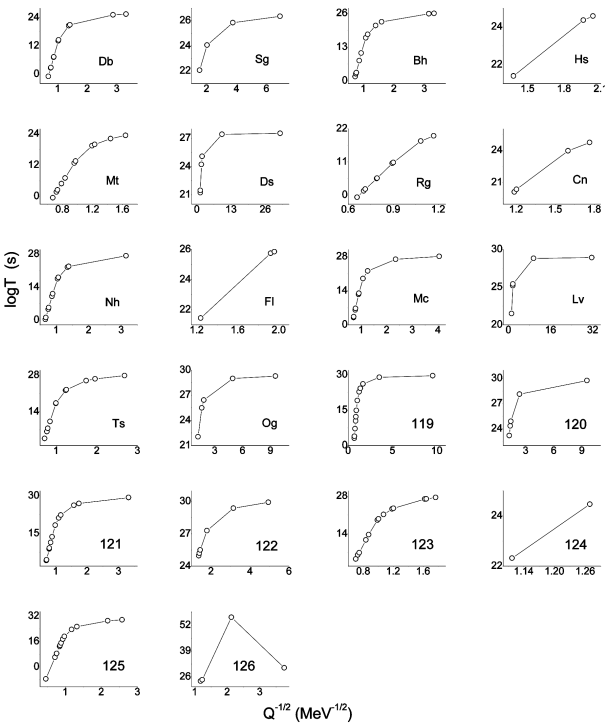

Fig. 2. Variation of logarithmic proton decay half-lives versus $1/\sqrt{Q}$

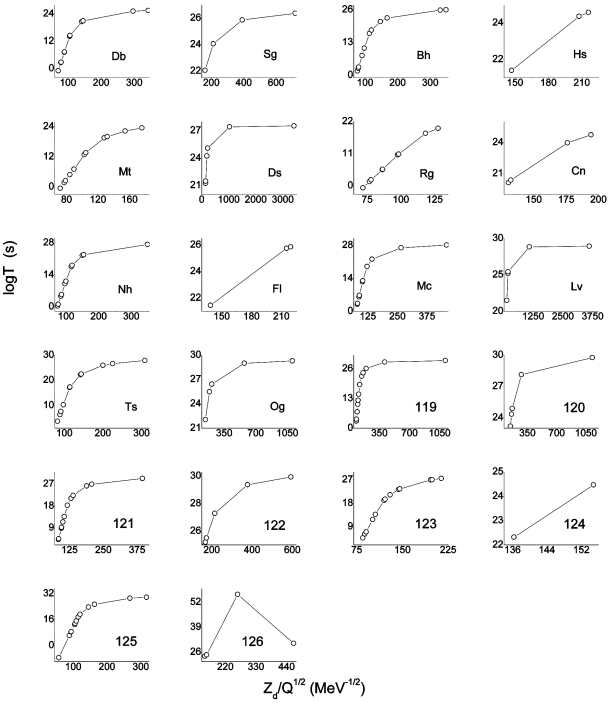

Fig. 3. Variation of logarithmic proton decay half-lives versus $Z_d/\sqrt{Q}$

Table 2. **Energy released, penetration factor, normalization factor, and logarithmic half-lives for proton decay in superheavy nuclei**

Nuclei	Q (MeV)	Penetration factor (P)	Normalization factor (F)	$\log T_{1/2}$
^{240}Rf	0.011	6.29×10^{-48}	7.56×10^{-02}	25.96
^{241}Db	2.131	5.45×10^{-21}	7.82×10^{-02}	–0.99
^{242}Db	1.711	1.48×10^{-24}	7.75×10^{-02}	2.58
^{243}Db	1.691	1.04×10^{-24}	7.72×10^{-02}	2.74
^{244}Db	1.341	4.5×10^{-29}	7.65×10^{-02}	7.1
^{245}Db	1.331	3.15×10^{-29}	7.63×10^{-02}	7.26
^{246}Db	0.961	4.92×10^{-36}	7.56×10^{-02}	14.07
^{247}Db	0.941	1.95×10^{-36}	7.54×10^{-02}	14.47
^{248}Db	0.531	1.84×10^{-42}	7.47×10^{-02}	20.5
^{249}Db	0.501	7.78×10^{-43}	7.45×10^{-02}	20.88
^{250}Db	0.121	4.38×10^{-47}	7.39×10^{-02}	25.13
^{251}Db	0.091	2.12×10^{-47}	7.37×10^{-02}	25.45
^{244}Sg	0.241	5.08×10^{-46}	7.58×10^{-02}	24.06
^{245}Sg	0.421	5.13×10^{-44}	7.57×10^{-02}	22.05
^{246}Sg	0.071	8.37×10^{-48}	7.51×10^{-02}	25.84
^{247}Sg	0.021	2.6×10^{-48}	7.48×10^{-02}	26.35
^{247}Bh	1.881	1.34×10^{-23}	7.73×10^{-02}	1.63
^{248}Bh	1.761	1.13×10^{-24}	7.69×10^{-02}	2.7
^{249}Bh	1.701	4.02×10^{-25}	7.66×10^{-02}	3.15
^{250}Bh	1.341	9.7×10^{-30}	7.6×10^{-02}	7.77
^{251}Bh	1.161	1.17×10^{-32}	7.55×10^{-02}	10.69
^{252}Bh	0.771	7.75×10^{-40}	7.49×10^{-02}	17.88
^{253}Bh	0.861	1.74×10^{-38}	7.48×10^{-02}	16.53
^{254}Bh	0.511	3×10^{-43}	7.42×10^{-02}	21.29
^{255}Bh	0.391	1.17×10^{-44}	7.39×10^{-02}	22.71
^{256}Bh	0.101	8.89×10^{-48}	7.34×10^{-02}	25.83
^{257}Bh	0.091	6.94×10^{-48}	7.32×10^{-02}	25.94
^{250}Hs	0.521	2.32×10^{-43}	7.55×10^{-02}	21.4
^{251}Hs	0.521	2.29×10^{-43}	7.53×10^{-02}	21.4
^{252}Hs	0.261	2.57×10^{-46}	7.48×10^{-02}	24.36
^{253}Hs	0.241	1.56×10^{-46}	7.45×10^{-02}	24.58
^{253}Mt	2.211	1.92×10^{-21}	7.7×10^{-02}	–0.53
^{254}Mt	1.851	1.83×10^{-24}	7.64×10^{-02}	2.5
^{255}Mt	1.931	1.15×10^{-23}	7.63×10^{-02}	1.7
^{256}Mt	1.611	7.6×10^{-27}	7.57×10^{-02}	4.88
^{257}Mt	1.431	5.41×10^{-29}	7.53×10^{-02}	7.03
^{258}Mt	1.091	9.34×10^{-35}	7.47×10^{-02}	12.8
^{259}Mt	1.051	1.63×10^{-35}	7.45×10^{-02}	13.56
^{260}Mt	0.701	2.12×10^{-41}	7.39×10^{-02}	19.45
^{261}Mt	0.661	6.23×10^{-42}	7.37×10^{-02}	19.98
^{262}Mt	0.481	3.77×10^{-44}	7.33×10^{-02}	22.2
^{263}Mt	0.371	2.06×10^{-45}	7.3×10^{-02}	23.46
^{256}Ds	0.581	3.6×10^{-43}	7.5×10^{-02}	21.21
^{257}Ds	0.561	2.03×10^{-43}	7.48×10^{-02}	21.46
^{258}Ds	0.321	3.6×10^{-46}	7.43×10^{-02}	24.21
^{259}Ds	0.241	4.98×10^{-47}	7.4×10^{-02}	25.08
^{260}Ds	0.001	1.85×10^{-49}	7.36×10^{-02}	27.51

The continuation of Table 2

Nuclei	Q (MeV)	Penetration factor (P)	Normalization factor (F)	$\log T_{1/2}$
^{262}Ds	0.011	2.29×10^{-49}	7.34×10^{-02}	27.42
^{259}Rg	2.301	3.1×10^{-21}	7.66×10^{-02}	–0.73
^{260}Rg	2.021	2.31×10^{-23}	7.61×10^{-02}	1.4
^{261}Rg	1.961	5.64×10^{-24}	7.58×10^{-02}	2.01
^{262}Rg	1.601	1.86×10^{-27}	7.52×10^{-02}	5.5
^{263}Rg	1.591	1.51×10^{-27}	7.5×10^{-02}	5.59
^{264}Rg	1.251	1.82×10^{-32}	7.44×10^{-02}	10.51
^{265}Rg	1.231	9.59×10^{-33}	7.42×10^{-02}	10.79
^{266}Rg	0.851	6.92×10^{-40}	7.36×10^{-02}	17.93
^{267}Rg	0.731	1.41×10^{-41}	7.33×10^{-02}	19.63
^{262}Cn	0.691	2.44×10^{-42}	7.46×10^{-02}	20.38
^{263}Cn	0.711	4.38×10^{-42}	7.44×10^{-02}	20.13
^{264}Cn	0.391	6.57×10^{-46}	7.39×10^{-02}	23.96
^{265}Cn	0.321	1.12×10^{-46}	7.37×10^{-02}	24.72
^{266}Nh	2.251	2.71×10^{-22}	7.58×10^{-02}	0.33
^{267}Nh	2.151	5.04×10^{-23}	7.55×10^{-02}	1.06
^{268}Nh	1.751	1.42×10^{-26}	7.49×10^{-02}	4.61
^{269}Nh	1.681	2.79×10^{-27}	7.46×10^{-02}	5.32
^{270}Nh	1.321	4.65×10^{-32}	7.41×10^{-02}	10.1
^{271}Nh	1.251	4.34×10^{-33}	7.38×10^{-02}	11.14
^{272}Nh	0.921	1.94×10^{-39}	7.33×10^{-02}	17.49
^{273}Nh	0.881	4.69×10^{-40}	7.31×10^{-02}	18.11
^{274}Nh	0.521	9.75×10^{-45}	7.26×10^{-02}	22.79
^{275}Nh	0.551	2.16×10^{-44}	7.24×10^{-02}	22.45
^{276}Nh	0.101	3.15×10^{-49}	7.18×10^{-02}	27.29
^{269}Fl	0.651	2.13×10^{-43}	7.39×10^{-02}	21.45
^{270}Fl	0.271	1.08×10^{-47}	7.34×10^{-02}	25.74
^{271}Fl	0.261	8.42×10^{-48}	7.32×10^{-02}	25.85
^{272}Mc	1.981	5.97×10^{-25}	7.51×10^{-02}	2.99
^{273}Mc	1.941	2.72×10^{-25}	7.48×10^{-02}	3.33
^{274}Mc	1.651	4.7×10^{-28}	7.43×10^{-02}	6.1
^{275}Mc	1.611	1.02×10^{-28}	7.41×10^{-02}	6.76
^{276}Mc	1.221	1.95×10^{-34}	7.36×10^{-02}	12.49
^{277}Mc	1.191	6.44×10^{-35}	7.33×10^{-02}	12.97
^{278}Mc	0.861	6.09×10^{-41}	7.29×10^{-02}	18.99
^{279}Mc	0.181	6.86×10^{-49}	7.21×10^{-02}	26.95
^{280}Mc	0.061	4.45×10^{-50}	7.18×10^{-02}	28.14
^{275}Lv	0.691	1.91×10^{-43}	7.36×10^{-02}	21.49
^{276}Lv	0.371	3.96×10^{-47}	7.31×10^{-02}	25.18
^{277}Lv	0.351	2.39×10^{-47}	7.29×10^{-02}	25.4
^{278}Lv	0.011	9.3×10^{-51}	7.24×10^{-02}	28.81
^{279}Lv	0.001	7.37×10^{-51}	7.22×10^{-02}	28.92
^{278}Ts	1.961	1.23×10^{-25}	7.46×10^{-02}	3.68
^{279}Ts	1.591	1.52×10^{-29}	7.41×10^{-02}	7.59
^{280}Ts	1.681	2.62×10^{-28}	7.4×10^{-02}	6.35
^{281}Ts	1.391	3.58×10^{-32}	7.35×10^{-02}	10.22
^{282}Ts	1.011	3.03×10^{-39}	7.3×10^{-02}	17.3
^{283}Ts	1.021	4.4×10^{-39}	7.28×10^{-02}	17.14
^{284}Ts	0.661	4×10^{-44}	7.23×10^{-02}	22.18

The continuation of Table 2

Nuclei	Q (MeV)	Penetration factor (P)	Normalization factor (F)	$\log T_{1/2}$
^{285}Ts	0.641	2.26×10^{-44}	7.21×10^{-02}	22.43
^{286}Ts	0.331	7.63×10^{-48}	7.17×10^{-02}	25.9
^{287}Ts	0.261	1.42×10^{-48}	7.15×10^{-02}	26.64
^{281}Og	0.691	5.47×10^{-44}	7.32×10^{-02}	22.04
^{282}Og	0.301	2.36×10^{-48}	7.26×10^{-02}	26.41
^{283}Og	0.391	2.04×10^{-47}	7.25×10^{-02}	25.47
^{284}Og	0.011	3.23×10^{-51}	7.2×10^{-02}	29.28
^{285}Og	0.041	6.11×10^{-51}	7.19×10^{-02}	29
^{284}119	2.001	7.96×10^{-26}	7.43×10^{-02}	3.87
^{285}119	2.091	4.82×10^{-25}	7.42×10^{-02}	3.09
^{286}119	1.681	4.64×10^{-29}	7.36×10^{-02}	7.11
^{287}119	1.421	2.43×10^{-32}	7.32×10^{-02}	10.39
^{288}119	1.171	8.18×10^{-37}	7.28×10^{-02}	14.87
^{289}119	1.311	4.14×10^{-34}	7.28×10^{-02}	12.16
^{290}119	0.941	5.62×10^{-41}	7.23×10^{-02}	19.03
^{291}119	0.661	1.15×10^{-44}	7.18×10^{-02}	22.73
^{292}119	0.531	3.52×10^{-46}	7.16×10^{-02}	24.24
^{293}119	0.361	4.99×10^{-48}	7.13×10^{-02}	26.09
^{295}119	0.081	7.72×10^{-51}	7.08×10^{-02}	28.9
^{296}119	0.011	1.65×10^{-51}	7.06×10^{-02}	29.57
^{287}120	0.641	4.03×10^{-45}	7.28×10^{-02}	23.17
^{288}120	0.491	7.88×10^{-47}	7.25×10^{-02}	24.88
^{289}120	0.541	2.78×10^{-46}	7.23×10^{-02}	24.34
^{291}120	0.181	4.68×10^{-50}	7.17×10^{-02}	28.12
^{292}120	0.011	1.09×10^{-51}	7.14×10^{-02}	29.75
^{290}121	2.021	3.61×10^{-26}	7.39×10^{-02}	4.22
^{291}121	1.981	1.81×10^{-26}	7.37×10^{-02}	4.52
^{292}121	1.581	9.49×10^{-31}	7.32×10^{-02}	8.8
^{293}121	1.561	3.91×10^{-31}	7.3×10^{-02}	9.19
^{294}121	1.411	2.48×10^{-33}	7.27×10^{-02}	11.39
^{295}121	1.571	7.27×10^{-31}	7.27×10^{-02}	8.92
^{296}121	1.271	1.25×10^{-35}	7.23×10^{-02}	13.69
^{297}121	1.031	3.22×10^{-40}	7.19×10^{-02}	18.28
^{298}121	0.831	4.28×10^{-43}	7.16×10^{-02}	21.16
^{299}121	0.741	3.02×10^{-44}	7.13×10^{-02}	22.31
^{300}121	0.401	4.15×10^{-48}	7.09×10^{-02}	26.17
^{301}121	0.331	7.66×10^{-49}	7.07×10^{-02}	26.91
^{302}121	0.091	3.25×10^{-51}	7.04×10^{-02}	29.28
^{303}121	0.091	3.19×10^{-51}	7.02×10^{-02}	29.29
^{294}122	0.481	1.94×10^{-47}	7.21×10^{-02}	25.5
^{295}122	0.531	6.69×10^{-47}	7.2×10^{-02}	24.96
^{296}122	0.311	3.14×10^{-49}	7.17×10^{-02}	27.29
^{297}122	0.511	3.91×10^{-47}	7.17×10^{-02}	25.19
^{298}122	0.041	7.28×10^{-52}	7.11×10^{-02}	29.93
^{299}122	0.101	2.62×10^{-51}	7.11×10^{-02}	29.37
^{297}123	2.031	1.38×10^{-26}	7.34×10^{-02}	4.64
^{298}123	1.881	4.21×10^{-28}	7.31×10^{-02}	6.15
^{299}123	1.791	6.53×10^{-29}	7.29×10^{-02}	6.96
^{300}123	1.431	1.1×10^{-33}	7.24×10^{-02}	11.74

The end of Table 2

Nuclei	Q (MeV)	Penetration factor (P)	Normalization factor (F)	$\log T_{1/2}$
$^{301}124$	1.311	1.21×10^{-35}	7.21×10^{-02}	13.7
$^{302}125$	0.871	4.07×10^{-43}	7.16×10^{-02}	21.18
$^{303}123$	0.371	6.91×10^{-49}	7.1×10^{-02}	26.95
$^{304}123$	1.021	5.25×10^{-41}	7.15×10^{-02}	19.07
$^{305}123$	0.991	1.82×10^{-41}	7.13×10^{-02}	19.53
$^{306}123$	0.691	2.15×10^{-45}	7.09×10^{-02}	23.46
$^{307}123$	0.711	3.66×10^{-45}	7.08×10^{-02}	23.23
$^{308}123$	0.381	8.03×10^{-49}	7.04×10^{-02}	26.89
$^{309}123$	0.321	1.92×10^{-49}	7.02×10^{-02}	27.51
$^{300}124$	0.801	2.94×10^{-44}	7.21×10^{-02}	22.32
$^{301}124$	0.621	2.1×10^{-46}	7.18×10^{-02}	24.46
$^{303}125$	1.391	7.81×10^{-35}	7.25×10^{-02}	12.89
$^{304}125$	1.151	2.04×10^{-39}	7.22×10^{-02}	17.47
$^{305}125$	1.051	4.02×10^{-41}	7.19×10^{-02}	19.18
$^{306}125$	4.651	2.12×10^{-14}	7.53×10^{-02}	–7.56
$^{307}125$	1.951	5.77×10^{-28}	7.25×10^{-02}	6.02
$^{308}125$	1.731	2.47×10^{-30}	7.21×10^{-02}	8.39
$^{309}125$	1.721	1.87×10^{-30}	7.2×10^{-02}	8.51
$^{310}125$	1.271	5.13×10^{-37}	7.14×10^{-02}	15.08
$^{311}125$	1.361	1.77×10^{-35}	7.14×10^{-02}	13.54
$^{312}125$	0.721	1.44×10^{-45}	7.07×10^{-02}	23.63
$^{313}125$	0.571	2.76×10^{-47}	7.04×10^{-02}	25.35
$^{314}125$	0.211	5.37×10^{-51}	7×10^{-02}	29.07
$^{315}125$	0.151	1.4×10^{-51}	6.98×10^{-02}	29.65
$^{308}126$	0.721	8.91×10^{-46}	7.15×10^{-02}	23.84
$^{309}126$	0.661	1.77×10^{-46}	7.13×10^{-02}	24.54
$^{310}126$	0.071	1.7×10^{-52}	7.06×10^{-02}	30.56

ferent decay modes such as the proton decay, spontaneous fission, and alpha decay for superheavy elements. From the detailed study of the comparison among the different decay modes, it is observed that the proton decay half-lives in the superheavy region are greater than that of alpha decay. For most of the superheavy nuclei, the proton decay half-lives are greater than that of spontaneous fission.

To check the Geiger–Nuttal law for the proton decay in superheavy nuclei, we have plotted the logarithmic proton decay half-lives versus $1/\sqrt{Q}$ (Fig. 2). It is found that the proton decay half-lives do not vary linearly with $1/\sqrt{Q}$. Figure 3 shows the variation of the logarithmic proton decay half-lives with $Z_d/\sqrt{Q}$. It is seen that the proton decay half-lives do not vary linearly with $Z_d/\sqrt{Q}$ as well. This fact clearly indicates that the proton decay does not follow the Geiger–Nuttal law.

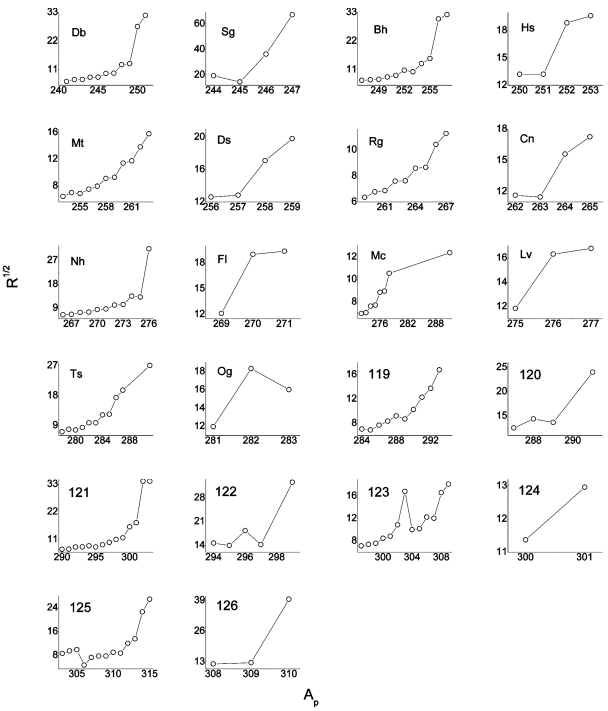

Fig. 4. Variation of $\sqrt{R}$ against mass number of the parent nuclei A

The nuclear charge radii can be derived from the proton decay half-lives. We have evaluated the nuclear charge radii using the semiempirical relation from [29]. Figure 4 shows the variation of $\sqrt{R}$ against the mass number of the parent nuclei. From this variation, we observe that the nuclear charge radii of superheavy nuclei do not vary systematically with the mass number of parent nuclei.

We have studied the proton decay in almost all superheavy nuclei with atomic numbers $Z = 104$–126 and found that the proton decay is possible in few superheavy nuclei (listed in Table 1). Proton decay half-lives are also longer than that of other decay modes. The competition of the proton decay with various decay modes such as the alpha decay and spontaneous fission reveals that the proton decay is not a dominant decay mode in the superheavy nuclei region. This means that the superheavy nuclei are stable against the proton decay.

1. M. Gonçalves, N. Teruya, O.A.P. Tavares, S.B. Duarte. Two-proton emission half-lives in the effective liquid drop model. *Phys. lett.* **774**, 14 (2017).

2. D.S. Delion, R.J. Liotta, R. Wyss. Theories of proton emission. *Phys. Reports* **424**, 113 (2006).
3. E. Maglione, L.S. Ferreira, R.J. Liotta. Proton emission from deformed nuclei. *Phys. Rev. C* **59**, R589(R) (1999).
4. M. DelSanto, Z. Meisel, D. Bazin, A. Becerril *et al.* β-delayed proton emission of ^{69}Kr and the ^{68}Se rp-process waiting point. *Phys. Lett. B* **738**, 453 (2014).
5. S.A. Alavi,V. Dehghani,M. Sayahi. Calculation of proton radioactivity half-lives. *Nucl. Phys. A* **977**, 49 (2018).
6. G. Raciti, M. De Napoli, G. Cardella, *et al.* Two-proton correlated emission from ^{18}Ne excited states. *Nucl. Phys. A* **834**, 464 (2010).
7. D. Baye, E.M. Tursunov. β delayed emission of a proton by a one-neutron halo nucleus. *Phys. Lett. B* **696**, 464 (2011).
8. W.F. Feix, E.R. Hilf. Nuclear proton emission predictions. *Phys. Lett. B* **120**, 14 (1983).
9. M. Anguiano, G. Co, A.M. Lallena. Photo-emission of two protons from nuclei. *Nucl. Phys. A* **744**, 168 (2004).
10. R. Coniglione, P. Sapienza, E. Migneco *et al.* High energy proton emission in heavy ion reactions close to the Fermi energy. *Phys. Lett. B* **471**, 339 (2000).
11. C. Giusti, F.D. Pacati. Two-proton emission induced by electron scattering. *Nucl. Phys. A* **535**, 573 (1991).
12. B. Ludewigt, R. Glasow, H. Löhner, R. Santo. Proton emission in a-induced reactions at 43 MeV nucleon. *Nucl. Phys. A* **408**, 359 (1983).
13. F. Guzmán, M. Gonçalves, O.A.P. Tavares *et al.* Proton radioactivity from proton-rich nuclei. *Phys. Rev. C* **59**, R2339(R) (1999).
14. D.S. Delion, R.J. Liotta, R. Wyss. Systematics of proton emission. *Phys. Rev. Lett.* **96**, 072501 (2006).
15. J.M. Dong, H.F. Zhang, G. Royer. Proton radioactivity within a generalized liquid drop model. *Phys. Rev. C* **79**, 054330 (2009).
16. E. Maglione, L.S. Ferreir. Proton emission from ^{125}Pm could be observed. *Phys. Rev. C* **94**, 044317 (2016).
17. P. Arumugam, L.S. Ferreira, E. Maglione. Proton emission, gamma deformation, and the spin of the isomeric state of ^{141}Ho. *Phys. Lett. B* **680**, 443 (2009).
18. S.B. Duarte, O.A.P. Tavares, F. Guzmán *et al.* Half-lives for proton emission, alpha decay, cluster radioactivity, and cold fission processes calculated in a unified theoretical framework. *Atomic Data and Nuclear Data Tables* **80**, 235 (2002).
19. L.S. Ferreira, E. Maglione, P. Ring. Self-consistent description of proton radioactivity. *Phys. Lett. B* **701**, 508 (2011).
20. D.S. Delion. *Theory of Particle and Cluster Emission* (Springer-Verlag, 2010).
21. https://www-nds.iaea.org/RIPL-3/
22. M. Kowal, P. Jachimowicz, J. Skalski. Ground State and Saddle Point: masses and deformations for even-even superheavy nuclei with $98 < Z < 126$ and $134 < N < 192$. arXiv:1203.5013
23. H.C. Manjunatha, B.M. Chandrika, L. Seenappa. Empirical formula for mass excess of heavy and superheavy nuclei. *Mod. Phys. Lett. A* **31** (28), 1650162 (2016).
24. G. Royer. Alpha emission and spontaneous fission through quasi-molecular shapes. *J. Phys. G: Nucl. Part. Phys.* **26**, 1149 (2000).
25. D.N. Poenaru, R.A. Gherghescu, W. Greiner. Single universal curve for cluster radioactivities and α decay. *Phys. Rev. C* **83**, 014601 (2011).
26. D. Ni, Z. Ren, T. Dong, C. Xu. Unified formula of half-lives for a decay and cluster radioactivity. *Phys. Rev. C* **78**, 044310 (2008).
27. V.Y. Denisov, A.A. Khudenko. α-decay half-lives: Empirical relations. *Phys. Rev. C* **79** (5), 054614 (2009).
28. C. Xu, Z. Ren, Y. Guo. Competition between α decay and spontaneous fission for heavy and superheavy nuclei. *Phys. Rev. C* **78**, 044329 (2008).
29. Y. Qian, Z. Ren, D. Ni. Attempt to probe nuclear charge radii by cluster and proton emissions. *Phys. Rev. C* **87**, 054323 (2013).
30. H.C. Manjunatha. Comparison of alpha decay with fission for isotopes of superheavy nuclei $Z = 124$. *Intern. J. Modern Phys. E* **25**, 1650074 (2016).
31. H.C. Manjunatha. Alpha decay properties of superheavy nuclei $Z = 126$. *Nucl. Phys. A* **945**, 42 (2016).
32. H.C. Manjunatha, K.N. Sridhar. Projectile target combination to synthesis superheavy nuclei $Z = 126$. *Nucl. Phys. A* **962**, 7 (2017).
33. H.C. Manjunatha, N. Sowmya. Competition between spontaneous fission ternary fission cluster decay and alpha decay in the super heavy nuclei of $Z = 126$. *Nucl. Phys. A* **969**, 68 (2018).
34. H.C. Manjunatha, N. Sowmya. Decay modes of superheavy nuclei $Z = 124$. *Inte Jou of Mod Phys E* **27** (5), 1850041 (2018).
35. N. Sowmya, H.C. Manjunatha. Competition between different decay modes in 279Ds. *DAE Symp. Nucl. Phys.* **63**, 200-201 (2018).
36. H.C. Manjunatha, K.N. Sridhar, N. Sowmya. Investigations of the synthesis of the superheavy element $Z = 122$. *Phys. Rev. C* **98**, 024308 (2018).
37. H.C. Manjunatha, K.N. Sridhar, N. Sowmya. Investigations on $^{64}\mathrm{Ni}+_Z\mathrm{An}^A \rightarrow_{Z=104-123}$ (SHN)$^{A=250-310}$ reactions. *Nucl. Phys. A* **987**, 382 (2019).
38. K.N. Sridhar, H.C. Manjunatha, H.B. Ramalingam. Search for possible fusion reactions to synthesize the superheavy element $Z = 121$. *Phys. Rev. C* **98** (6), 064605 (2018).
39. H.C. Manjunatha, K.N. Sridhar. Investigation to synthesis more isotopes of superheavy nuclei $Z = 118$. *Nucl. Phys. A* **975**, 136 (2018).
40. N. Sowmya, H.C. Manjunatha. Competition between different decay modes of superheavy element $Z = 116$ and synthesis of possible isotopes. *Braz. J. Phys.* **49**, 874 (2019).
41. N. Sowmya, H.C. Manjunatha. A Study of Binary Fission and Ternary Fission in $^{232-238}$U. *Bulg. J. Phys.* **46**, 16 (2019).

42. G.R. Sridhar, H.C. Manjunatha, N. Sowmya, P.S.D. Gupta, H.B. Ramalingam. Atlas of cluster radioactivity in actinide nuclei. *Europ. Phys. J. Plus* **135** (3), 291 (2020).

43. M.G. Srinivas, H.C. Manjunatha, K.N. Sridhar, N. Sowmya, A.C. Raj. Proton decay of actinide nuclei. *Nucl. Phys. A* **995**, 121689 (2020).

44. N. Sowmya, H.C. Manjunatha, N. Dhananjaya, A.M. Nagaraja. Competition between binary fission, ternary fission, cluster radioactivity and alpha decay of 281Ds. *J. Radioanalyt. Nucl. Chem.* **323** (3), 1347 (2020).

Received 12.08.19

М.Г. Срінівас, Х.К. Манджуната,
К.Н. Шрідхар, А.К. Радж, П.С. Дамодара Гупта

СИСТЕМАТИЧНЕ ДОСЛІДЖЕННЯ ПРОТОННОГО РОЗПАДУ НАДВАЖКИХ ЕЛЕМЕНТІВ

Розглядається протонний розпад майже всіх надважких ядер з атомними номерами $Z = 104$–126. Розраховано енергію, що вивільняється в такому розпаді (Q_P), коефіцієнт проникнення (P), коефіцієнт нормування (F) та періоди напіврозпаду. Останні більші, ніж для інших каналів розпаду, таких як альфа-розпад та спонтанне ділення. У порівнянні з іншими каналами розпаду, протонний розпад не є домінуючим в області надважких ядер. Це означає, що надважкі ядра можна вважати стабільними відносно протонного розпаду.

Ключові слова: радіоактивність, надважкі ядра, протонний розпад.